

Original Article

Effects of targeted nano-delivery systems combined with hTERT-siRNA and Bmi-1-siRNA on MCF-7 cells

Lei Liu*, Huixiang Li, Min Zhang, Xinquan Lv

Department of Pathology, Basic Medical College, Henan Key Laboratory for Tumor Pathology, Zhengzhou University, Henan Province, China. *Equal contributors.

Received March 16, 2015; Accepted May 17, 2015; Epub June 1, 2015; Published June 15, 2015

Abstract: The aim of this study was to evaluate the efficiency of a targeted siRNA nano-delivery system to silence the expression of Bmi-1 and hTERT, and to verify the toxicity of this delivery system in MCF-7 breast cancer cells. The most effective Bmi-1 siRNA and hTERT siRNA sequences were selected using RT-PCR and Western blotting. The polyethyleneimine (PEI)/siRNA nano-condensate was synthesized using PEI and modified using an NGR peptide fragment for targeting to tumor cells. The vector morphology, particle size and zeta potential were observed using an atomic force microscope and a laser particle size analyzer. The MCF-7 breast cancer cell line was transfected with the vector, and cytotoxicity was tested by MTT assays. The transfection efficiency was evaluated by qRT-PCR and Western blotting. Changes in gene expression and apoptosis rate were measured by flow cytometry. The size of LPN carrier and the condensate particle was between 100 and 200 nm and the potentials were close to neutral. There was maximum transfection efficiency and no significant increase in toxicity at 15 pmol/L. Bmi-1 and hTERT expression decreased, but the inhibition rate increased in the hTERT siRNA group, the hTERT+Bmi-1 siRNA group and the hTERT+Bmi-1 siRNA group compared with the scrambled siRNA group and the control group. Moreover, the hTERT+Bmi-1 siRNA group had the highest level of gene silencing. The complex, composed of Lipo, PEI and siRNA, is low toxicity and efficient transfection vectors. The expression level of Bmi-1 and hTERT was decreased by the gene silencing of either Bmi-1 or hTERT, but the effects were more significant when both were silenced simultaneously.

Keywords: Breast cancer, MCF-7, nano-delivery system, Bmi-1, PEI, siRNA

Introduction

Tumor occurrence and development requires the activation of many pro-oncogenes and the inactivation of many tumor suppressor genes. Bmi-1 (B cell-specific Moloney leukemia virus integration site-1) was the first gene discovered in the polycomb protein family, and it plays an important role in cell immortalization and differentiation and embryonic stem cell development [1]. Bmi-1 is highly expressed in a variety of human tumors, including lung cancer, ovarian cancer, acute myelogenous leukemia, nasopharyngeal cancer, breast cancer, and neuroblastoma, suggesting that Bmi-1 may play an important role in cancer occurrence and development [2-4]. Studies have shown that Bmi-1 is important for maintaining proliferation and self-renewal of neural stem cells, hematopoietic stem cells, and cancer stem cells [3]. P16INK4A

and P19ARF (P14ARF in humans) are two tumor suppressor genes encoded by INK4a-ARF and inhibited by Bmi-1. P16INK4a can directly inhibit cell proliferation by inhibiting Rb phosphorylation and preventing cells from entering S phase (DNA synthesis phase). P19ARF can prevent the inactivation of p53, which induces cell growth arrest, senescence and apoptosis. Bmi-1 can also induce downstream expression of hTERT, which prevents cell aging and results in immortalization. Studies have shown that Bmi-1 is expressed in 85% of invasive breast ductal carcinomas [4] and that it is highly expressed in a variety of breast cancer cell lines [5]. Bmi-1 expression is also associated with the Hedgehog signaling pathway, which regulates of human mammary stem cell self-renewal [6].

Telomeres are composed of 1000-2000 untranscribed DNA repeat sequences (TTAGGG) that

form a protective cap on chromosome ends to prevent fusion and degradation [9, 10]. Telomerase is excessively activated in most of tumors and is involved in the regulation of cell cycle proteins, such as p16Ink4a and p21WAF1, which induce epithelial cell apoptosis [7]. Studies have shown that Bmi-1 and hTERT are closely associated in some cell lines [8]. hTERT is a rate-limiting factor in telomerase activity regulation but is not the only factor that can inhibit p16Ink4a/(Rb) protein activation [9]; both E6 and Bmi-1 can activate hTERT in breast cancer cell lines [8]. Therefore, Bmi-1 and hTERT may inhibit apoptosis through different pathways and affect the expression levels of other genes in return.

To solve the problems of low siRNA transfection efficiency and degradation by nucleases, we used Lipid-polycation-nucleic acid (LPN) complex nanocarrier vectors. The nanocarrier system is a new transport system that has been used in recent years to transport biological macromolecules, including peptides, proteins, oligonucleotides and therapeutic genes. The nanocarrier system have the advantages of being highly efficient, non-immunogenic, safe, inexpensive, biodegradable and stable compared with other gene carriers, and it is expected to have significant potential in gene transfer and gene therapy. Polyethylenimine (PEI) is the most extensively studied polycation vector in recent years, and it can be condensed with nucleic acid molecules to form nanocarriers. Liposomes are used to envelope the PEI/DNA (RNA) nanocarriers to form LPN complexes, which have a structure similar to a virus, with a nucleus containing genetic material and a lipid shell [10]. LPN can improve the transfection efficiency by effectively promoting its integration with the cell membrane and protecting nucleic acid and cationic polymers from nucleic acid enzymes. To reduce PEI/RNA toxicity and improve their accumulation at the tumor site, the LPN surface was further modified using NGR peptide fragments, which are specifically recognized by aminopeptidase N (CD13); CD13 is also highly expressed in tumor tissues and cells [11]. Several studies have shown that NGR also specifically binds to integrin $\alpha\beta 3$ [12], which is primarily expressed during angiogenesis [13], further improving NGR's ability to target tumor angiogenesis.

Materials and methods

Cell line and cell culture

As previously described [14], breast carcinoma cell line MCF-7 cells were maintained in RPMI-1640 medium (Gibco, USA) supplemented with 10% fetal bovine serum (FBS) (HyClone Laboratories, Logan, USA), 100 U/ml penicillin and 100 $\mu\text{g}/\text{ml}$ streptomycin at 37°C in the presence of 5% CO_2 .

Preparation of Lipo/PEI/siRNA complexes

The target siRNA was added to Tris-HCl buffer at 100 $\mu\text{g}/\text{mL}$. The PEI/siRNA suspension was obtained by adding the appropriate amount of PEI. The particle sizes and zeta potentials were then measured. A total of 20 μmol POPC, DDAB, DSPE-PEG2000 and DSPE-PEG200-maleimide were dissolved in a chloroform/methanol mixture, and then a lipid film was formed by allowing the solution to evaporate and dry in a vacuum. After the PEI/siRNA suspension and lipid film were mixed, the solution was vortexed for 5 min and ultrasonically processed for 30 min to generate the LPN complex.

A polypeptide CNGRCK2HK3HK11 was added to the LPN complex suspension under stirring, and this mixture was maintained at room temperature overnight to obtain a polypeptide with a modified sequence containing NGR-LPN complexes (NGR/LPN).

Morphology, particle size and zeta potential measurements

The PEI/siRNA condensate was mixed with the N/P = 10 and NGR/LPN complex suspension, then spotted onto mica, coated and dried. Finally, each complex was investigated using a SPM-9500J3 Atomic Force Microscope (AFM) (Shimadzu Corporation, Japan) in the contact mode.

The particle sizes of PEI/siRNA condensate, LPN and NGR/LPN compound were analyzed using a Nano-ZS90 laser particle size analyzer. The refractive index was set to 1.590, the absorption coefficient to 0.010, the temperature to 25°C, and the measurement mode was set to Auto. The PEI/condensate was measured directly after the LPN and NGR/LPN complexes

Nano-delivery system in MCF-7 cells

Table 1. The size and zeta potential of PEI/siRNA complex and LPN/siRNA complex

	PEI/Bmi-1 siRNA	LPN/Bmi-1 siRNA	PEI/hTERT siRNA	LPN/hTERT
Size (nm)	128.6 ± 1.2	156.2 ± 1.8	119.5 ± 3.5	150.5 ± 2.7
Zeta potential	21.1 ± 0.4	2.8 ± 0.1	20.2 ± 1.3	2.8 ± 0.7

were measured after a 15-fold dilution. The average Z value was set as the result of the measurements. The zeta potential of the PEI/siRNA condensate, LPN and NGR/LPN complexes was measured using the Nano-ZS90 laser particle size analyzer. The dielectric constant was set to 79, the viscosity coefficient to 0.8872, the temperature to 25°C, and the measurement mode was set to Auto. The PEI/siRNA condensate was measured directly, whereas the LPN and NGR/LPN complexes were measured after a 15-fold dilution. Each sample was measured three times.

Verification of encapsulated LPN complexes and anti-restriction assay

A total of 5 µl heparin was mixed with 100 µl prepared LPN compound, then 20 µl was removed as a reserve. RNA enzyme was added to the remaining suspension and incubated for 1 h at 37°C and blocked with 0.25 mol/L EDTA. After Genefinder staining and 1% agarose gel electrophoresis, the result was analyzed using a gel imaging system.

RNA enzyme solution was added to the siRNA and NGR/LPN suspension, incubated for 1 h at 37°C and terminated by adding 0.25 mol/L EDTA. Heparin was then added. After Genefinder staining and 1% agarose gel electrophoresis, the result was analyzed using a gel imaging system.

Liposome stability assays

The prepared LPN compound was observed for 2 weeks. The changing state, particle diameter and potential were continuously measured. Nucleic acid release from the LPN complexes was examined by electrophoresis analysis.

siRNA synthesis and cell transfection

Small interference RNA (siRNA) sequences were synthesized by Genescript, Shanghai. The siRNA sequences were as follows:

Bmi-1-homo-692: 5'-CC-GACCACUACUGA-AUAUTT-3', Bmi-1-homo-933: 5'-GGAUCG-GAAAGUAAACAAATT-3', Bmi-1-homo-1071: 5'-CCAGAUUGAUGUC-

AUGUAUTT-3', hTERT-homo-1522: 5'-GGCACCA-AGAAGUUCAUTT-3', hTERT-homo-1798: 5'-G-GAGCAAGUUGCAAAGCAUTT-3', hTERT-homo-2-860: 5'-GCACCAACAUCUACAAGAUUTT-3', hTERT-homo-1788: 5'-GGAAGAGUGUCUGGAGCAATT-3', Scrambled sequence: 5'-UUCUCCGAACGUGUCACGUTT-3'.

MCF-7 cell lines were transfected with Lipofectamine 2000 (Invitrogen) according to the manufacturer's instructions and divided into 9 groups, Negative control group (NC), PEI group, Bmi-1 siRNA group (G1), hTERT siRNA group (G2), Bmi-1 siRNA LPN (G3), hTERT siRNA LPN group (G4) and hTERT+Bmi-siRNA group (G5).

Cell growth inhibition rate

The cell growth inhibition rate was described previously [15]. Briefly, the cells were inoculated in 96-well culture plates at 5,000 cells/well and treated according to their specific group. The Cell Counting kit-8 (CCK-8) solution (Beyotime Institute of Biotechnology) was added at 24, 48 and 72 h in the siRNA group in different groups, prior to incubation for 2 h. Following incubation, the absorbance (ABS) of each sample was measured at 450 nm. Inhibition Rate (IR) = (ABS of experimental group-ABS of scramble group)/ABS of scramble group × 100%.

RNA isolation, semi-quantitative RT-PCR and Western blotting

RNA isolation, semi-quantitative RT-PCR was performed as described previously [14]. In brief, total RNAs were extracted by TRIzol reagent (Invitrogen) according to the manufacturer's instructions, and then subjected to first-strand cDNA synthesis with AMV first strand DNA synthesis kit (Biotech Co., Shanghai, P.R. China). Primers were used to amplify the specific band using the procedures described as follows: initial denaturation at 94°C for 2 min, followed by 30 sec at 94°C, 30 sec at different genes annealing temperatures, and 30 sec at

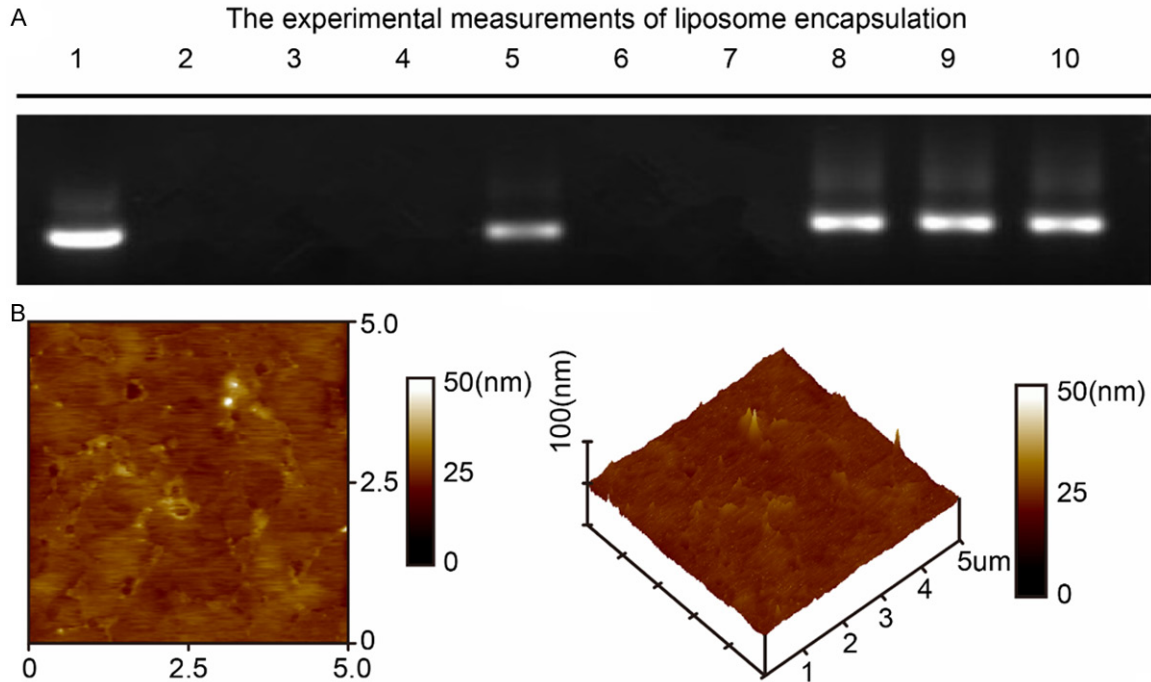


Figure 1. A. Electrophoresis of LPN complexes on PEI/siRNA encapsulation condensate (1, small interference RNA 2, RNA enzyme-digested siRNA 3, PEI/siRNA condensate 4, RNA enzyme-digested PEI/siRNA condensate 5, RNA enzyme-digested PEI/siRNA condensate plus heparin 6, LPN complex 7, RNA enzyme-digested LPN complex 8, RNA enzyme-digested LPN complex plus heparin 9, RNA enzyme-digested LPN complex plus heparin and Triton X-100 10, RNA enzyme-digested LPN complex plus heparin and Triton X-100). B. Plane view of the LPN complex analyzed by atomic force microscopy, C. 3D view of the LPN compound analyzed by atomic force microscopy.

72°C for a total of 30 cycles and a terminal extension at 72°C for 6 min. After amplification, 10 µl of PCR products were resolved on a 1% agarose gel. DNA bands were visualized by UV light and documented with a Gene Tools (Model P67UA). Semi-quantitative analysis of Band intensity was performed with Gene Tools software (UVP, Inc., Upland, USA). The primers used are as follows: hTERT (Homo sapiens) forward primer 5'-AAATGCGGCCCTGTTTCT-3' and reverse primer 5'-CAGTGCCTTGTGAGGAGCA-3', Bmi-1 (Homo sapiens) forward primer 5'-CCA-CCTGATGTGTGCTTTG-3' and reverse primer 5'-TTCAGTAGTGGTCTGGTCTTGT 3', GAPDH (Homo sapiens) forward primer 5'-GGGGCTCTCC-AGAACATCATCC-3' and reverse primer 5'-ACG-CCTGCTTACCACCTTCTT-3'. All experiments were performed in triplicate.

Western blotting was performed as described previously [14]. The primary antibodies and dilutions used are as follows: hTERT (1:1000, Abcam, Co), Bmi-1 (1:500; Santa Cruz, Co), and GAPDH (1:5000; Millipore, Co). Primary antibodies were applied, followed by horseradish-peroxidase-conjugated secondary antibodies. For detection, DAB solution was used to devel-

op the bands of specific proteins on the membranes according to manufacturer's instructions. Quantification of band intensity was performed using Gene Tools (UVP, Inc.).

Cell apoptosis detection

MCF-7 cells in specific groups were trypsinized, washed with cold PBS buffer, and then resuspended in PBS buffer, respectively. Annexin V-FITC (BD Biosciences, USA) at final concentration of 1 µg/ml and 250 ng of propidium iodide were added to a mixture containing 100 µl of cell resuspension and binding buffer (BD Biosciences) each. After cells were vortexed and incubated for 15 min at room temperature (RT) in the dark, 400 µl of binding buffer was added to the mixture for flow cytometric analysis. CellQuest software was used for acquisition and analysis of the data, and the percentage of cell apoptosis was determined.

Statistical analysis

For cell proliferation, cell apoptosis, RT-PCR, Western blotting, values were obtained from three independent experiments as described

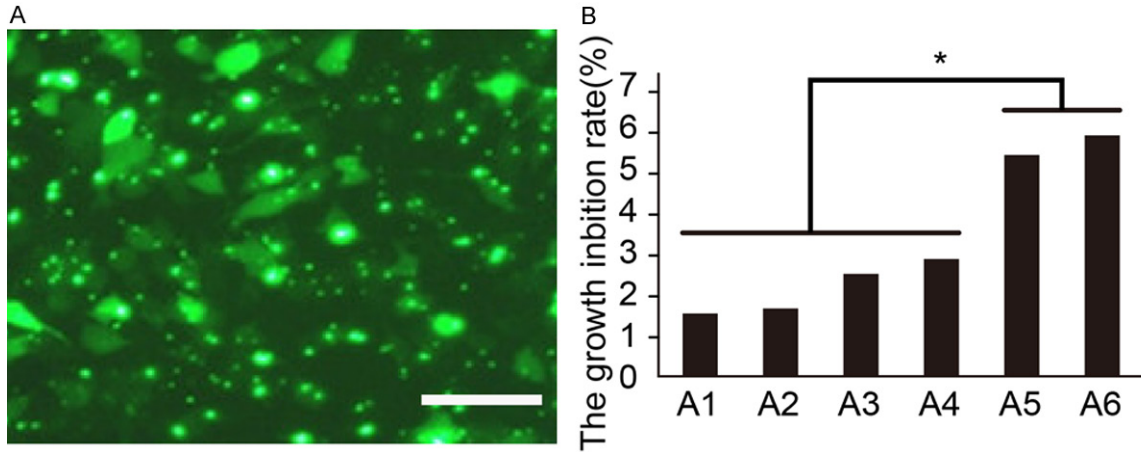


Figure 2. A. Image of MCF-cell transfection efficiency (Scale bar, 20 μ m). B. Inhibition rate (%) of LPN nanocarriers on MCF-7 cells.

Table 2. Inhibition rate (%) of LPN nanocarriers on MCF-7 cells

Group	N	Average inhibition rate (%)	F	P
A1 (2 pmol)	3	1.62	82.381	0.000
A2 (5 pmol)	3	1.76		
A3 (10 pmol)	3	2.58		
A4 (15 pmol)	3	2.85		
A5 (20 pmol)	3	5.42		
A6 (25 pmol)	3	5.89		

above. The data were performed by one-way analysis and LSD-t test of variance using SPSS version 13.0 (SPSS, Chicago, USA). Quantitative variables were expressed as the means \pm standard deviations. In the statistical analyses, a $P < 0.05$ was considered statistically significant and all P -values were two-sided.

Results

The size, zeta potential and morphology of PEI/siRNA complex and LPN/siRNA complex

To examine the differences between LPN nanocarrier and condensate, a Nano-ZS90 laser particle size analyzer was carried out to measure the relative sizes and zeta potentials. Post-analysis revealed that the PEI/Bmi-1 siRNA and LPN/Bmi-1 siRNA diameters were 128.6 ± 1.2 and 156.2 ± 1.8 nm, respectively, and their potentials were 21.1 ± 0.4 and 2.8 ± 0.1 , respectively (Table 1). PEI/hTERT siRNA and LPN/hTERT siRNA exhibited the same trend

in size and potential. The PEI/hTERT siRNA and LPN/hTERT siRNA diameters were 119.5 ± 3.5 and 150.5 ± 2.7 nm, respectively, and their potentials were 20.2 ± 1.3 and 2.79 ± 0.7 , respectively. The nanocarrier size was between 100 and 200 nm, and its potential was close to neutral (about -20~20). The experimental measurements of liposome encapsulation were shown in Figure 1A. The morphology of the LPN nanocarrier was also detected by atomic force microscopy (Figure 1B, 1C).

Transfection concentration optimization

To find out the optimal RNAi transfection concentration, MCF-7, human breast cancer cell line, was selected to be treated with RNA interference. We investigated LPN nanocarrier uptake by confocal microscopy in MCF-7 cell lines (Figure 2A). Experiment was classified into 6 groups except the negative group (Table 2). To examine the influence of LPN on the growth rate of MCF-7 cell lines, CCK8 assay was performed. The growth inhibition rate in groups A5 and A6 was significant ($P < 0.01$), especially group A6 (Table 2; Figure 2B). Interestingly, when we adjusted the concentration to 15 pmol, optimal transfection efficiency and minimal toxicity were observed.

Down-regulation of Bmi-1 and hTERT

Next, we examined whether Bmi-1 protein and mRNA expression in MCF-7 cells decreased upon treatment with Bmi-1 siRNA. Compared to the negative, PEI, G1 and G2 groups, the Bmi-1

Nano-delivery system in MCF-7 cells

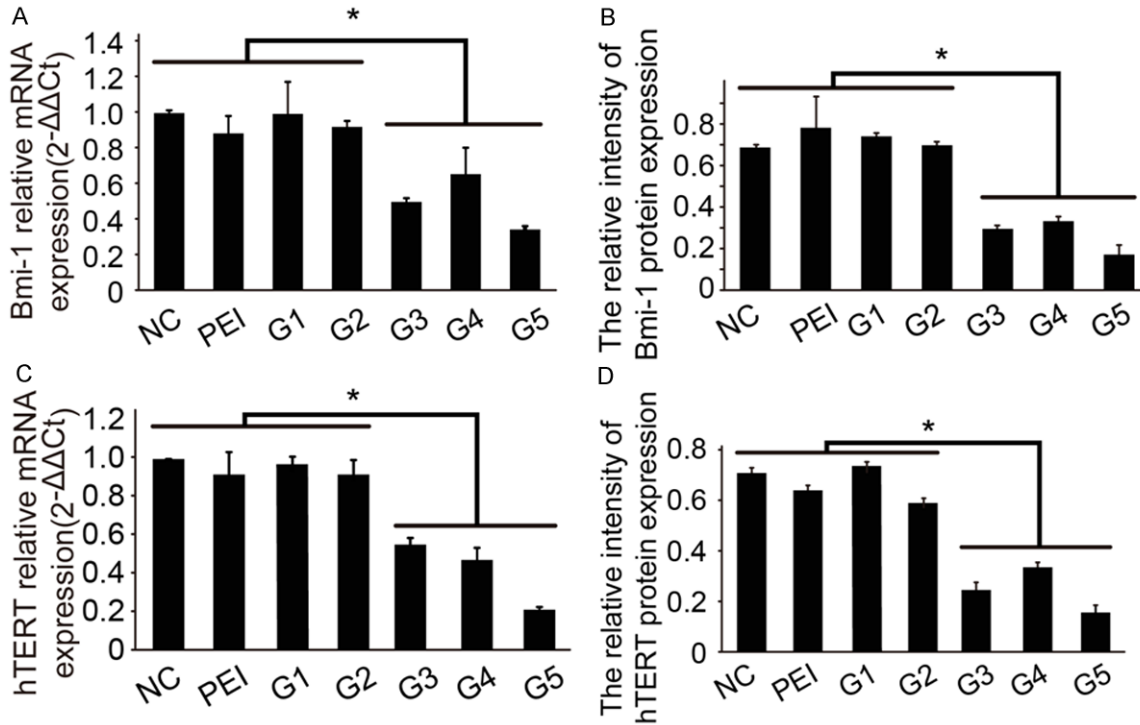


Figure 3. A and B. Bmi-1 mRNA and protein expression level was decreased in MCF-7 cells after siRNA transfection. C and D. hTERT mRNA and protein expression level was downregulated in MCF-7 cell.

protein and mRNA expression level in groups G3, G4 and G5 was down-regulated significantly (**Figure 3A, 3B**). Similarly, hTERT protein and mRNA expression level in hTERT siRNA-transfected MCF-7 cell lines also decreased, particularly in group G5 (**Figure 3C, 3D**).

Bmi-1 and hTERT siRNA affect cell growth rate and apoptosis

We next examined whether Bmi-1 or hTERT siRNA exerted effects on MCF-7 cellular function. It was found that the cellular growth rate was significantly decreased in Bmi-1 siRNA-transfected and hTERT siRNA-transfected cells ($P < 0.01$, **Figure 4A**), which was most apparent in group G5. In addition, the proportion of apoptosis in G3, G4 and G5 was significantly increased (**Figure 4B, 4C**).

Discussion

This study primarily evaluated Bmi-1 and hTERT siRNA effects on the mRNA level. Through MTT, apoptosis analysis, qRT-PCR and WB, we demonstrated that silencing of either gene can significantly affect the other's mRNA expression level and reduce senescence and apoptosis in MCF-7 cells. Moreover, silencing both mRNAs

has a time-dependent synergistic effect on MCF-7 cells. We used polycation nanocarriers to improve the transfection efficiency. The nanocarrier complex combined with the GRE (CNGRCK2HK3HK11) end to enhance siRNA targeting. Compared to liposomal transfection alone, the polycation nanocarrier group had a higher transfection rate and lower toxicity.

Bmi-1 is highly expressed in a variety of tumors, stem cells and cancer stem cells [16]. As an important growth factor, Bmi-1 overexpression can cooperate with c-myc to increase telomerase activity [17] and decrease p16INK4a and p19AFR expression in epithelial cells, which allow the cells to escape cell death [3]. Tátrai et al [18] activated Bmi-1 and hTERT by lentiviral transduction, which immortalized the cells without disturbing other biological characteristics. After several generations, the cells did not show any signs of senescence. Transfection of Bmi-1 into MCF-7 cells inhibited cell proliferation, induced apoptosis and reduced hTERT expression. This phenomenon was consistent with previous studies. As a PCG family member, Bmi-1 plays an important role in tumor treatment and provides a crucial therapeutic target.

Nano-delivery system in MCF-7 cells

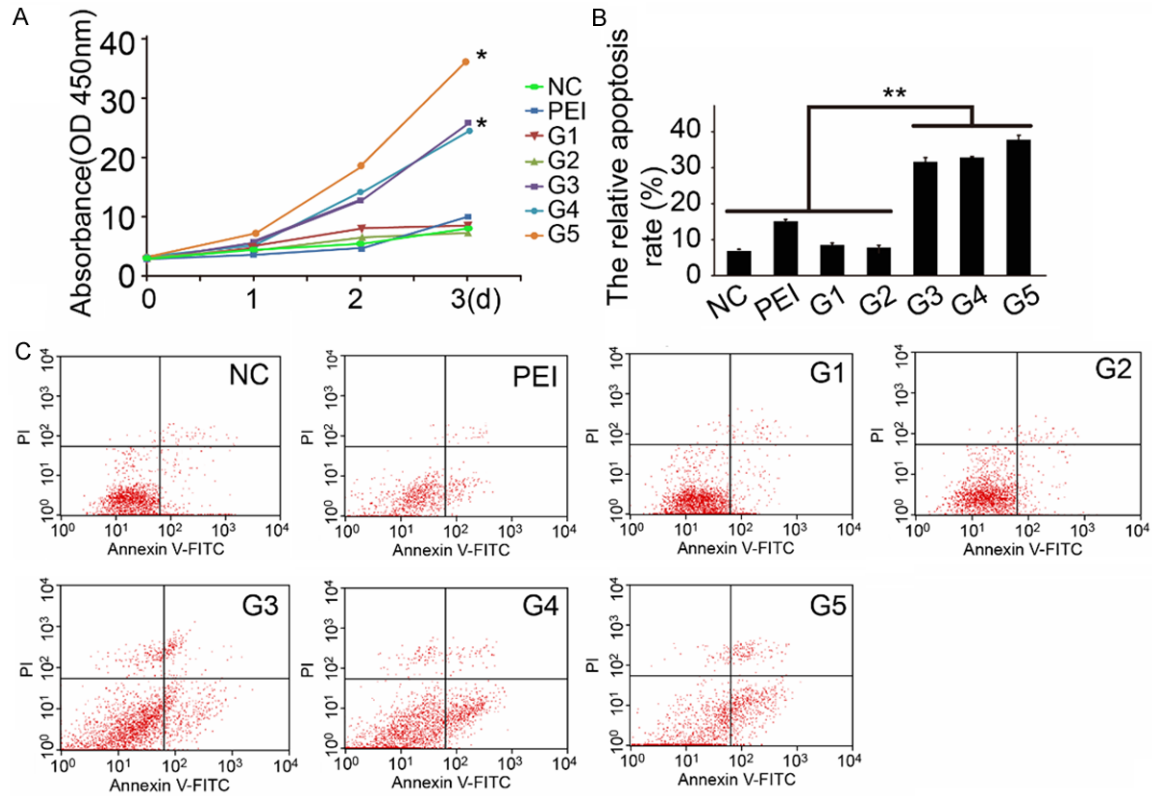


Figure 4. A. The comparison of cell growth inhibition rates in different groups in MCF-7 breast cancer cells. B. The relative apoptosis rate in different groups. C. The apoptosis of cancer cells were analyzed by flow cytometry.

Telomerase is a reverse transcriptase DNA synthesis enzyme that synthesizes the lost DNA during cell division using RNA template and stably maintaining the telomere length. Telomerase is activated in most tumor cells, and telomerase activation may be one of most critical gene changes in tumor occurrence and progression. Telomerase activity is primarily regulated at the transcriptional level. Thus, hTERT is a limiting factor in regulating telomerase's activity, which is consistent with hTERT's expression level. However, more than 90% malignant tumor cells have high hTERT expression and telomerase activity. Bmi-1 and hTERT are key genes in maintaining tumor cell self-renew and proliferation. Previous studies have suggested that Bmi-1 and hTERT affect telomerase expression through distinct but synergistic ways. However, the mechanism by which Bmi-1 regulates telomerase activity remains unknown. Moreover, how telomerase affects Bmi-1 has not been extensively studied. In the experiment, we found that silencing hTERT also affects Bmi-1 expression. This is likely because some hTERT gene targets may affect Bmi-1 expression. Silencing of both critical genes (Bmi-1 and

hTERT) can inhibit tumor cell proliferation and induce apoptosis. This combination has a larger effect than silencing a single gene as it likely affects two important signaling pathways at the same time.

In preliminary studies, we generated a small effect by liposomal siRNA transfection. Thus, we adopted a novel nanocarrier approach to increase transfection efficiency. Chumakova et al [19] first combined the PEI and DNA to generate a complex with similar transfection efficiency to and lower toxicity than other transfection materials. Due to its high specificity for angiogenic processes, the NGR subunit has been used in drug therapies, including attachment to viral particles and cytokines, to induce apoptosis [20, 21]. We had previously synthesized NGR/PEI/ASON complexes for gene silencing and obtained satisfactory outcomes [22]. However, ASON is more stable than siRNA. Wu et al [23] previously synthesized PEI/siRNA complexes to silence CD44v6 expression in cancer cells and generated stable siRNA transfection nanocarriers. In this current study, we improved on our previous efforts with the gen-

eration of the NGR/PEI/ASON vector, which has superior transfection efficiencies. However, there are several limitations in our approach. With regard to the two widely expressed crucial genes, we investigated their effects on only one breast cancer cell line because of the lack of resources to investigate their roles in other breast cancer cell lines and tumor cells. In this study, the state of post-silencing remains unknown. Furthermore, the expression level of the nanocarrier's CD13 amino acid residues was low in MCF-7 cells, and the affinity of NGR was lower than the high CD33 expression cell lines. According to recent studies, both Bmi-1 and hTERT are expressed in breast cancer stem cells. Activation of both genes immortalized the cells. In our future research, we will confirm the relationship between Bmi-1 and hTERT in breast cancer stem cells.

In conclusion, co-silencing of Bmi-1 and hTERT may be an effective treatment for breast cancer. Our study confirmed that Bmi-1 and hTERT expression can affect the other's expression, but the mechanism remains unknown.

Acknowledgements

This work was supported by the grants from National Natural Science Foundation of China (No. 90406024).

Disclosure of conflict of interest

None.

Address correspondence to: Dr. Huixiang Li, Department of Pathology, Henan Key Laboratory for Tumor Pathology, Basic Medical College, Zhengzhou University, 40 Daxue Road, Zhengzhou 450001, Henan, China. E-mail: lihuixiang19@126.com

References

- [1] Kim JH, Yoon SY, Jeong SH, Kim SY, Moon SK, Joo JH, Lee Y, Choe IS and Kim JW. Overexpression of Bmi-1 oncoprotein correlates with axillary lymph node metastases in invasive ductal breast cancer. *Breast* 2004; 13: 383-388.
- [2] Sawa M, Yamamoto K, Yokozawa T, Kiyoi H, Hishida A, Kajiguchi T, Seto M, Kohno A, Kitamura K, Itoh Y, Asou N, Hamajima N, Emi N and Naoe T. BMI-1 is highly expressed in M0-subtype acute myeloid leukemia. *Int J Hematol* 2005; 82: 42-47.
- [3] Song LB, Zeng MS, Liao WT, Zhang L, Mo HY, Liu WL, Shao JY, Wu QL, Li MZ, Xia YF, Fu LW, Huang WL, Dimri GP, Band V and Zeng YX. Bmi-1 is a novel molecular marker of nasopharyngeal carcinoma progression and immortalizes primary human nasopharyngeal epithelial cells. *Cancer Res* 2006; 66: 6225-6232.
- [4] Cui H, Hu B, Li T, Ma J, Alam G, Gunning WT and Ding HF. Bmi-1 is essential for the tumorigenicity of neuroblastoma cells. *Am J Pathol* 2007; 170: 1370-1378.
- [5] van der Lugt NM, Domen J, Linders K, van Roon M, Robanus-Maandag E, te Riele H, van der Valk M, Deschamps J, Sofroniew M, van Lohuizen M. Posterior transformation, neurological abnormalities, and severe hematopoietic defects in mice with a targeted deletion of the bmi-1 proto-oncogene. *Genes Dev* 1994; 8: 757-769.
- [6] Leung C, Lingbeek M, Shakhova O, Liu J, Tanger E, Saremaslani P, Van Lohuizen M and Marino S. Bmi1 is essential for cerebellar development and is overexpressed in human medulloblastomas. *Nature* 2004; 428: 337-341.
- [7] Ramirez RD, Morales CP, Herbert BS, Rohde JM, Passons C, Shay JW and Wright WE. Putative telomere-independent mechanisms of replicative aging reflect inadequate growth conditions. *Genes Dev* 2001; 15: 398-403.
- [8] Dimri GP, Martinez JL, Jacobs JJ, Keblusek P, Itahana K, Van Lohuizen M, Campisi J, Wazer DE and Band V. The Bmi-1 oncogene induces telomerase activity and immortalizes human mammary epithelial cells. *Cancer Res* 2002; 62: 4736-4745.
- [9] Kiyono T, Foster SA, Koop JI, McDougall JK, Galloway DA and Klingelutz AJ. Both Rb/p16INK4a inactivation and telomerase activity are required to immortalize human epithelial cells. *Nature* 1998; 396: 84-88.
- [10] Tagawa T, Manvell M, Brown N, Keller M, Perouzel E, Murray KD, Harbottle RP, Teclé M, Booy F, Brahimi-Horn MC, Coutelle C, Lemoine NR, Alton EW and Miller AD. Characterisation of LMD virus-like nanoparticles self-assembled from cationic liposomes, adenovirus core peptide mu and plasmid DNA. *Gene Ther* 2002; 9: 564-576.
- [11] Corti A and Ponzoni M. Tumor vascular targeting with tumor necrosis factor alpha and chemotherapeutic drugs. *Ann N Y Acad Sci* 2004; 1028: 104-112.
- [12] Mizuguchi H, Koizumi N, Hosono T, Utoguchi N, Watanabe Y, Kay MA and Hayakawa T. A simplified system for constructing recombinant adenoviral vectors containing heterologous peptides in the HI loop of their fiber knob. *Gene Ther* 2001; 8: 730-735.

Nano-delivery system in MCF-7 cells

- [13] Liu L, Anderson WF, Beart RW, Gordon EM and Hall FL. Incorporation of tumor vasculature targeting motifs into moloney murine leukemia virus env escort proteins enhances retrovirus binding and transduction of human endothelial cells. *J Virol* 2000; 74: 5320-5328.
- [14] Xu Z, Liu H, Lv X, Liu Y, Li S and Li H. Knockdown of the Bmi-1 oncogene inhibits cell proliferation and induces cell apoptosis and is involved in the decrease of Akt phosphorylation in the human breast carcinoma cell line MCF-7. *Oncol Rep* 2011; 25: 409-418.
- [15] Lv X, Pang X, Jin X, Song Y and Li H. knockdown enhances the effects of fluorouracil in the breast cancer cell line MDA-MB-468. *Biomed Rep* 2014; 2: 910-914.
- [16] Park IK, Qian D, Kiel M, Becker MW, Pihalja M, Weissman IL, Morrison SJ and Clarke MF. Bmi-1 is required for maintenance of adult self-renewing haematopoietic stem cells. *Nature* 2003; 423: 302-305.
- [17] Ball AJ and Levine F. Telomere-independent cellular senescence in human fetal cardiomyocytes. *Aging Cell* 2005; 4: 21-30.
- [18] Tatrai P, Szepesi A, Matula Z, Szigeti A, Buchan G, Madi A, Uher F and Nemet K. Combined introduction of Bmi-1 and hTERT immortalizes human adipose tissue-derived stromal cells with low risk of transformation. *Biochem Biophys Res Commun* 2012; 422: 28-35.
- [19] Chumakova OV, Liopo AV, Andreev VG, Cicenaitė I, Evers BM, Chakrabarty S, Pappas TC and Esenaliev RO. Composition of PLGA and PEI/DNA nanoparticles improves ultrasound-mediated gene delivery in solid tumors in vivo. *Cancer Lett* 2008; 261: 215-225.
- [20] van Laarhoven HW, Gambarota G, Heerschap A, Lok J, Verhagen I, Corti A, Toma S, Gallo Stampino C, van der Kogel A and Punt CJ. Effects of the tumor vasculature targeting agent NGR-TNF on the tumor microenvironment in murine lymphomas. *Invest New Drugs* 2006; 24: 27-36.
- [21] Curnis F, Arrigoni G, Sacchi A, Fischetti L, Arap W, Pasqualini R and Corti A. Differential binding of drugs containing the NGR motif to CD13 isoforms in tumor vessels, epithelia, and myeloid cells. *Cancer Res* 2002; 62: 867-874.
- [22] Zhou T, Jia X, Li H, Wang J, Zhang H, A Y and Zhang Z. New tumor-targeted nanosized delivery carrier for oligonucleotides: characteristics in vitro and in vivo. *Int J Nanomedicine* 2011; 6: 1527-1534.
- [23] Wu Y, Wang W, Chen Y, Huang K, Shuai X, Chen Q, Li X and Lian G. The investigation of polymer-siRNA nanoparticle for gene therapy of gastric cancer in vitro. *Int J Nanomedicine* 2010; 5: 129-136.